ABSTRACT

Mechanics of Lithospheric Delamination in Extensional Settings

Jeffrey A. Jex, M.S.

Chairman: John A. Dunbar, Ph.D.

Delamination, the foundering of the lower crust and sub-crustal lithosphere, is one of the most important geodynamic processes that is still poorly understood. Geodynamic modeling has constrained conditions and likely outcomes of delamination in orogenically-thickened crust. In this study, I do the same for delamination in extensional settings by using finite element models of young passive margins. Delamination in these models may occur as melt beneath oceanic crust intrudes between the lower continental crust and sub-crustal lithosphere, driven by buoyancy. When sufficient melt is available and the lower crust is weak, the melt wedges between the lower crust and sub-crustal lithosphere, initiating delamination of the sub-crustal lithosphere. The speed of delamination is strongly dependent on weakness of the lower crust followed by the amount of melt present.

Mechanics of Lithospheric Delamination in Extensional Settings

by

Jeffrey A. Jex, B.S.

A Thesis

Approved by the Department of Geology

_____

Stacy C. Atchley, Ph.D., Chairperson

Submitted to the Graduate Faculty of
Baylor University in Partial Fulfillment of the
Requirements for the Degree
of

Master of Science

Approved by the Thesis Committee

_____

John A. Dunbar, Ph.D., Chairperson

_____

Robert Jay Pulliam, Ph.D.

_____

Ronald B. Morgan, Ph.D.

Accepted by the Graduate School

May 2015

_____

J. Larry Lyon, Ph.D., Dean

Page bearing signatures is kept on file in the Graduate School.

TABLE OF CONTENTS

LIST OF FIGURES

LIST OF TABLES

ACKNOWLEDGMENTS

Foremost I would like to express my sincere gratitude to my advisor, Dr. John Dunbar, for his guidance, support, and thoughtful remarks. I would also like to acknowledge my other committee members, Dr. Jay Pulliam and Dr. Ron Morgan for their valuable insights and time. I would like to thank my family for their support throughout my entire university career. I would like to thank my brother Jay Jex for reminding me just how interesting geoscience can be.

DEDICATION

To my loving wife Asenath, who has given me encouragement and motivation through this graduate school adventure; I could never have done this without her. I also dedicate it secondly to my daughter Hazel, whose cheery temperament and smile have helped me immeasurably along the path towards graduation.

CHAPTER ONE

Introduction

This study was conducted to determine the feasibility of, and conditions necessary for, delamination of the sub-crustal lithosphere in extensional tectonic environments, such as rift zones. The possibility of delamination in such environments has been proposed, and a specific case of it has been modeled, but it has generally received little attention. This study opens up the possibility of delamination to an entirely new setting, volcanic passive margins, and gives first order constraints on what conditions would lead to, or have caused, delamination in such settings.

CHAPTER TWO

Manuscript One

Mechanics of Lithospheric Delamination in Extensional Settings

Delamination, the foundering of the lower crust and sub-crustal lithosphere, is one of the most important geodynamic processes that is still poorly understood. Little direct evidence exists for lithospheric delamination, but petrologic constraints and geophysical evidence indicate it has occurred in a range of tectonic settings. However, geodynamic modeling has constrained conditions and likely outcomes of delamination in orogenically-thickened crust [*Schott and Schmeling*, 1998; *Ueda et al.*, 2012; *Krystopowicz and Currie*, 2013]. In this study, I do the same for delamination in extensional settings by means of finite element modeling of young passive margins. Passive margins develop as continents become extended beyond the point of breaking. Melt produced during the rifting process intrudes between the lower continental crust and sub-crustal lithosphere, driven by buoyancy. When sufficient melt is available and the lower crust is weak, the melt wedges between the lower crust and sub-crustal lithosphere, initiating delamination of the sub-crustal lithosphere. The speed of delamination is strongly dependent on weakness of the lower crust, followed by the amount of melt present.

1. Introduction

The primary geodynamic processes of plate motion are subduction, sea-floor spreading and transform motion [*Forsyth and Uyedaf*, 1975]. Lithospheric delamination

may be another important force for plate motion, although it is currently poorly understood, with little direct evidence of its occurrence [*Anderson*, 2007]. Delamination also appears to have a significant impact on the long-term behavior of the continental lithosphere [*Bajolet et al.*, 2012].

In typical continental lithosphere, the lower crust is weak and has low viscosity, whereas the upper mantle lithosphere is strong. This is sometimes referred to as the "jelly sandwich model" (Figure 1) [*Burov*, 2011]. The juxtaposition of low and high viscosity material makes the lower crust/sub-crustal lithosphere boundary an easy site for decoupling, if it is sufficiently weak [*Leech*, 2001; *Semprich and Simon*, 2014].

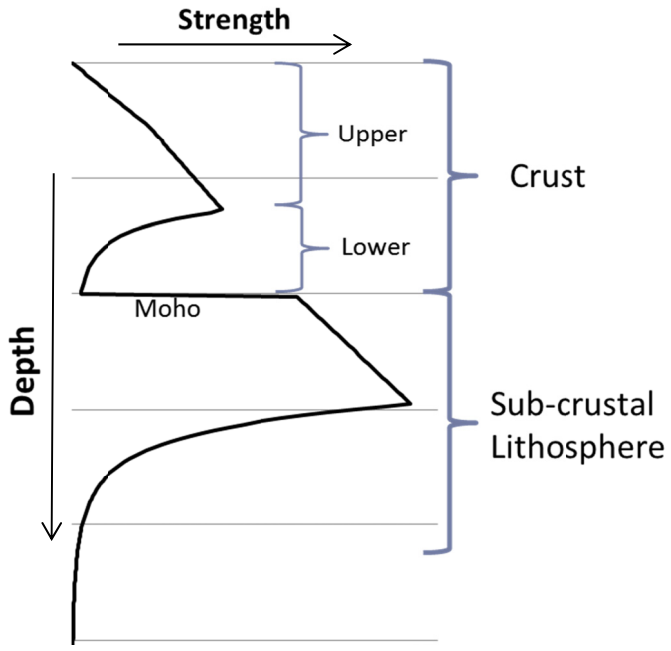

Figure 1. Initial strength of 40 km thick continental crust and sub-crustal lithosphere. The amount of weak lower crust is directly proportional to the amount of total crust, meaning thicker crust has a larger window of weak lower crust. The strength of the lithosphere is primarily controlled by temperature and pressure; the base is typically near 120-130 km, around 1300°C.

Lithospheric delamination is thought to occur as the sub-crustal lithosphere develops density instability, with denser rocks in the lithosphere than the asthenosphere. When a suitable decoupling zone is available, the lower crust and sub-crustal lithosphere "peel" off, somewhat reminiscent of a subduction zone [*Bird*, 1979]. The term lithospheric delamination most commonly refers to this "peeling" off of the lower crust and upper-mantle lithosphere near the Moho, leaving behind the upper and middle crust in contact with asthenosphere below [*Morency and Doin*, 2004; *Valera et al.*, 2011]. An alternative mechanism for lithospheric recycling is removal of sub-crustal lithosphere in Rayleigh-Taylor drips, formed by convective instabilities in the asthenosphere or at density instabilities occurring at continental rifts [*Houseman et al.*, 1981; *Jull and Kelemen*, 2001].

Localities where delamination is thought to have occurred include Tibet [*Bird*, 1978; *Ren and Shen*, 2008], Colorado Plateau [*Bird*, 1979], Western Mediterranean [*Channell and Mareschal*, 1989], Andes [*Kay and Mahlburg-Kay*, 1991], Alboran sea [*Seber et al.*, 1996; *Calvert et al.*, 2000; *Valera et al.*, 2008], Sierra Nevada mountains [*Ducea and Saleeby*, 1998; *Zandt et al.*, 2004], Basin and Range [*Meissner and Mooney*, 1998], Alps [*Meissner and Mooney*, 1998], Variscan Belt [*Arnold et al.*, 2001], Vrancea region [*Knapp et al.*, 2005], Eastern Anatolia [*Göğüş and Pysklywec*, 2008a], Rwenzori Mountains [*Wallner and Schmeling*, 2010], and Morocco [*Bezada et al.*, 2014].

Most delamination research has focused on thickening orogenic roots pushing rocks in to the eclogite stability field. Eclogitized mafic crust tends to be 50-300 kg/m^3 denser than the asthenosphere. In a standard continental geotherm, eclogitization starts near 40-60 km [*Krystopowicz and Currie*, 2013]. Eclogite formation in the lower crust is

a likely mechanism by which a density contrast significant enough to decouple the lower crust and upper mantle from the rest of the crust might occur. Delamination without the presence of eclogite is harder to explain [*Kay and Mahlburg-Kay*, 1991]. Delamination of a dense underplate as opposed to orogenically thickened crust also likely occurs [*Thybo and Artemieva*, 2013]. Some workers have postulated ideas about delamination in zones of extension. One possibility is that an asthenospheric upwelling could accumulate below crust or thin lithosphere, eventually creating an underplate of eclogite which might delaminate vertically [*Meissner and Mooney*, 1998]. The Basin and Range province of North America is greatly extended, and sometime in the past an underplate layer may have delaminated, leaving behind the current thin crust [*Thybo and Artemieva*, 2013].

Delamination requires the sub-crustal lithosphere to be denser than the underlying asthenosphere. As discussed by Poudjom Djomani et al. [2001], sub-crustal lithosphere buoyancy in relation to asthenosphere depends on pressure, temperature and composition, where composition is mainly controlled by age. Archean and Proterozoic sub-crustal lithospheres with typical geotherms are positively buoyant with respect to the Asthenosphere. Phanerozoic sub-crustal lithosphere is positively buoyant in areas of basaltic volcanism with hot geotherms. However, in older areas that have cooled to a steady-state geotherm, Phanerozoic sub-crustal lithosphere is negatively buoyant (Phanerozoic sub-crustal density range: 3280-3360 kg m-^{3}). This sub-crustal lithosphere could delaminate if a suitable delamination plane is available and a gap or conduit for upwelling asthenosphere exists, or forms, to allow initiation of delamination.

The sub-crustal lithosphere is strong because it is cooler than the underlying asthenosphere. The lower temperatures are also the cause for the density instability of the

sub-crustal lithosphere. In normal continental lithosphere, the negative buoyancy of the sub-crustal lithosphere is offset by the positive buoyancy of the crust. Hence, the only thing preventing delamination is the strength of the lower crust. Any mechanism that reduces the strength of the lower crust, without significantly heating the sub-crustal lithosphere would likely causes delamination [*Morency and Doin*, 2004].

The occurrence of delamination has been suggested mostly on the basis of petrologic evidence, and rarely (though increasingly) through geophysical evidence [*Calvert et al.*, 2000; *Fillerup et al.*, 2010; *Giacomuzzi et al.*, 2011; *Bezada et al.*, 2014]. The continental crust has an andesitic bulk composition, which requires a large ultramafic complement at the base of the continental crust. The ultramafic complement is frequently missing, and may have delaminated into the mantle [*Kay and Mahlburg-Kay*, 1991; *Rudnick*, 1995]. Uplift may commonly be induced by delamination. Once the dense crust and sub-crustal lithosphere delaminate, the remaining crust isostatically rebounds [*Meissner and Mooney*, 1998; *Chiarabba and Chiodini*, 2013]. A sudden increase in mafic volcanism might imply decompressional melting of asthenosphere and possibly melt from the delaminated block [*Ducea*, 2011].

Geophysical observations supporting the occurrence of delamination are mostly based on seismic, and occasionally on gravity, methods. The typical seismic signature of delamination shows asthenosphere (shallow, sub-crustal slow anomaly) under thin crust, with detached lithosphere nearby (fast anomaly). Anomalies with sharp edges for the upwelling asthenosphere and shallower delaminated lithosphere are thought to be indicative of erosion by advection, as opposed to thermal erosion, which would produce gradational boundaries, and a more diffuse anomaly [*Bezada et al.*, 2014]. In some cases

the lithosphere appears to have delaminated as a single coherent mass [*Fillerup et al.*, 2010]; in other cases piecewise delamination seems to have occurred [*Bezada et al.*, 2014].

A handful of finite element models have been created to model delamination, most of which have focused on delamination in thickened crust, usually in compressional structural regimes. Models have predicted delamination involving the peeling off of large slabs, as well as weaker events, where delamination shuts down after a small portion breaks away [*Schott and Schmeling*, 1998; *Krystopowicz and Currie*, 2013]. Past models created for delamination in extensional settings have been for relatively small scale, specific cases [*Wallner and Schmeling*, 2010, 2011], although delamination is thought to have occurred over a broad area in the Basin and Range [*Thybo and Artemieva*, 2013] .

Passive margins form when continents are pulled apart, and often include the generation of large amounts of melt [*Geoffroy*, 2005]. As the continent is stretched, instead of extreme thinning, the extending continental crust is intruded by dikes, which make up for some of the material deficit from extension. Once the continent breaks apart, a new oceanic spreading center is formed at the rift axis [*Scrutton*, 1982]. The relative size of the transition zone between normal continental crust and the continent-ocean boundary varies, but is generally much sharper than other types of margins (30-100 km) [*Franke*, 2013]. Volcanic passive margins are known for having enormous volumes of melt, both on the surface and as underplates in the subsurface [*White and McKenzie*, 1989]. The end result is continental lithosphere forming a sharp boundary zone with very young and thin oceanic lithosphere (~ 7 km), which are both underlain by hot (> 1300 °C) asthenosphere.

Mantle melt forms dense magma, which may pond at the Moho, creating an underplate [*Fyfe*, 1992; *Thybo and Artemieva*, 2013]. Based on laboratory experiments and seismic velocity analysis, the density of mantle melt is 2700-3000 g cm^{-3}. Melt near 3000 g cm^{-3}, when driven purely by buoyancy, would accumulate along the Moho, decoupling the crust from the sub-crustal lithosphere and creating an underplate. Such an underplate, under the proper conditions (generally depths greater than 30 km) may crystallize into a gabbro-peridotite-anothosite complex, which has the potential to delaminate because of its high density, similar to eclogite in an orogenic root [*Fyfe*, 1992]. Certain volcanic passive margins have been observed to have a thick, 15-20 km underplate (northern Grenville Province, Eastern Canadian Shield, [*Funck et al.*, 2011]). The North Atlantic margin also appears to have mafic intrusions as an underplate, or sills [*White et al.*, 2008]; similarly, the Baikal Rift Zone has sills [*Thybo and Artemieva*, 2013]. It was observed that large volumes of magma intrude into the North Atlantic continental ocean transition zone, 540-600 km^3 for every 1 km along strike [*White et al.*, 2008]. Either by sills, a single underplate layer, or both- many passive margins show signs of large amounts of mafic intrusion [*White and McKenzie*, 1989; *Thybo and Artemieva*, 2013]. On the other hand, non-volcanic margins exist where crust has become extremely thin, and no volcanism has occurred [*Lavier and Manatschal*, 2006; *Tucholke et al.*, 2007].

In this study, I model possible delamination processes in a zone of continual extension, a passive margin, using finite element code. I hypothesize that a dense mafic melt might intrude into the lower crust at a passive margin, decoupling the crust from the sub-crustal lithosphere by lowering the viscosity of the lower crust with the addition of

melt, and by severing the weak bond between viscous lower crust and strong sub-crustal lithosphere. This mafic melt emplacement may allow dense Phanerozoic sub-crustal lithosphere to peel off, beginning along the rift axis, and progressively moving landward, without a need for eclogite or any other dense mineral to start delamination, but solely by weakening the coupling of the sub-crust lithosphere to the lower crust. An ALE (arbitrary Lagrangian-Eulerian) finite element code, Picses2D (Particle In Cell Solid Earth Simulator, in 2D), models emplacement of dense melt at a young passive rifted margin, potentially inducing delamination of the sub-crustal lithosphere. Model results show that the weakness of the lower crust is the prime determinant of delamination initiation, followed by the amount of initial melt, and, thirdly, by the amount of additional melt supplied while delamination is in progress (where more melt speeds up the delamination process). The initial mechanism of delamination, intrusion of melt at a volcanic margin, has never before been modeled, but style of delamination, by decoupling lower crust and sub-crustal lithosphere is similar to models already published.

2. Methods

I use numerical experiments to study the possibility of delamination in extensional settings. The numerical modeling method is limited by the capabilities of the code used and processing power available, but has advantages over analog methods in that numerical inputs and outputs are easily extracted at any stage in the experiment. Numerical methods also make it possible to more closely represent the wide range of material properties and forces involved in geodynamic processes at the correct spatial and temporal scales.

2.1. Governing Equations

On geologic timescales, the lithosphere and asthenosphere deform at slow rates, such that inertial forces can be neglected. Inertial forces are minor compared to those of gravity and viscous resistance, the former being 10^{23} times smaller than the latter [*Gerya*, 2010]. The momentum conservation equation, with inertial effects ignored, is:

$$\nabla \cdot \sigma + \rho \mathrm{g} = 0, \tag{1}$$

where σ is the Cauchy stress tensor, ρ is the mass density and g is the acceleration from gravity. The flow is assumed to be incompressible, therefore volume is conserved. This is achieved by the continuity equation which enforces incompressibility:

$$\nabla \cdot v = 0, \tag{2}$$

where v is flow velocity. For the problem to be closed, the stress tensor σ must be related to velocity and pressure: $\sigma = \sigma(v, p)$. The stress tensor resolved into its hydrostatic (or spherical) stress σ^P and the deviatoric stress σ^D is

$$\sigma = \sigma^P + \sigma^D, \tag{3}$$

where hydrostatic stress σ^P is:

$$\sigma^P = \frac{1}{3} Tr[\sigma], \tag{4}$$

where $Tr[\sigma]$ is the trace of the stress tensor, σ. Pressure, P, is the negative of hydrostatic stress, $P = -\sigma^P$. In Newtonian fluids, where viscosity is constant and the fluid is incompressible, the deviatoric stress tensor σ^D is related to the velocity gradient through dynamic viscosity η as follows:

$$\sigma^D = 2\eta\dot{\epsilon}, \tag{5}$$

where $\dot{\epsilon}$ is the strain rate tensor:

$$\dot{\epsilon} = \frac{1}{2}(\nabla v + (\nabla v)^T). \tag{6}$$

Equations (1), (2), (3), (5), and (6) form a closed set, and yield the following formulation of the Stokes equation [*Thieulot*, 2011]:

$$\nabla \cdot (\eta \nabla v) - \nabla P + \rho g = 0, \quad (7)$$

where v is velocity, and P is pressure.

2.1.1. *Heat transport equation*

Temperature affects material density, viscosity, and phase. The temperature is computed in this system by solving the heat transport equation, as follows:

$$\rho c_p \left(\frac{\partial T}{\partial t} + v \cdot \nabla T \right) = \nabla \cdot (k \nabla T) + A, \quad (8)$$

where T is temperature, k is thermal conductivity, c_p is heat capacity and A is radiogenic heat production. For a full treatment of Stokes flow and the heat transport equation, the reader is referred to *Gerya* [2010].

2.2. Material models

Materials are modeled after one of the following viscosity laws: linear viscous, visco-plastic, or a combination of temperature and strain rate dependent power-law viscous, Byerlee's law Mohr-column-plastic and Brace and Kohlsedt lithosphere with diffusion creep [*Byerlee*, 1978; *Brace and Kohlstedt*, 1980; *Buffett and Becker*, 2012; *Van Wijk et al.*, 2008]. The lithosphere converts from a dislocation creep model to a diffusion creep model below depths of 130 km (Table 1; Table 2).

Dislocation and diffusion creep are dominant at relatively high temperatures and high stresses, diffusion creep occurs in the deep mantle [*Gerya*, 2010]. Dislocation creep occurs in the upper mantle, by migration of imperfections in the crystalline lattice. The result of dislocation creep is a non-linear, non-Newtonian viscosity. It is a type of power-law rheology, and can be modeled as:

Table 1. General parameters used in all models

Meaning	Value
Coefficient of thermal expansion (K^{-1})	3.00×10^{-5}
Adiabatic temperature gradient (K km^{-1})	3.00 x 10-^{4}
Acceleration due to gravity (m s-^{2})	9.81
Max viscosity (Poise)	1.00×10^{23}
Min viscosity (Poise)	1.00×10^{17}
Density for Byerlee's law (kg m-^{3})	1000

Table 2. Material parameters

Meaning	Asthenosphere	Upper Crust[a]	Entire crust[b]	Upper Mantle	Oceanic crust	Lower Crust[a]	Underplate (solid)	Underplate (melt)	Eclogitized underplate
Reference Density (g km-^{3})	3300	2750	2800	3300	2950	2850	3000	3000	3700
Heat conductivity (W m^{-1} K^{-1})	3.5	2.5	2.5	3.5	2.25	2.5	2.25	2.25	2.25
Specific heat capacity (J K^{-1})	1250	875	875	1250	850	875	850	850	850
Heat production rate (W m^{-3})	0	7.50×10^{8}	7.50×10^{8}	0	0	7.50×10^{8}	0	0	0
Flow law (see table 4)	linear, 1×10^{19} [c]	Wet Quartzite	Wet Granite	Dry Olivine	Plagioclase An_{75}	Plagioclase An_{75}	Plagioclase An_{75}	linear, $1e10^{17}$ [c]	Plagioclase An_{75}

[a] only used for models with a two layer crust; [b] Used for sensitivity test models; [c] flow is constant linear viscous, values in Poise.

$$\dot{\varepsilon} = A_D \sigma^n \exp\left[-\frac{E_a}{RT}\right], \quad (9)$$

where $\dot{\varepsilon}$ is strain rate, σ is stress, T is absolute temperature, R is the Boltzmann gas constant, and A_D, n and E_a are empirically determined rheological parameters, which are, respectively, the material constant, the stress exponent, and activation energy.

Peierls creep, also called "stress limiter" or "low-temperature plasticity", occurs at relatively low temperatures. It occurs due to stress-assisted, thermally activated motion of crystalline dislocations. Peierls creep allows for slab bending better than power-law creep and is more sensitive to stress, but less sensitive to temperature, than power-law creep[*Kameyama et al.*, 1999]. Peierls creep is typically used to model the lithosphere. Peierls creep is modeled as follows:

$$\dot{\varepsilon} = A \exp\left[-\frac{E_a}{RT}\left(1 - \frac{\sigma}{\sigma_p}\right)^q\right], \quad (10)$$

where A and q are material constants, E_a is activation enthalpy of the glide motion over the Peierls hill, and σ_p is the Peierls stress. Initial tests using Peierls creep showed the parameters to be poorly constrained in this study, and instead the sub-crustal lithosphere was modeled with the hybrid visco-plastic described above.

The lithosphere is modeled with several mechanisms in series, Byerlee's law, Mohr-column-plastic [*Byerlee*, 1978], Brace and Kohlsedt lithosphere [*Brace and Kohlstedt*, 1980] and includes a pseudo-plastic mechanism for the lower ductile lithosphere [*Buffett and Becker*, 2012]. Once below depths greater than 130 km the lithosphere model converts solely to diffusion creep [*Van Wijk et al.*, 2008](Table 3) to account for the low viscosities from dislocation creep at high mantle temperatures. These rheology types are in series, meaning the weakest rheology takes over at any given conditions, except below 130 km depths, where diffusion creep is dominant.

Table 3. Parameters for diffusion creep, after [*Van Wijk et al.*, 2008]

Parameter	Value
PT depth (km)	130
Reference viscosity (Pa s)	1.00×10^{19}
Activation energy (J mol^{-1})	2.60×10^{5}
Activation volume (m^3/s)	1.58×10^{13}
Reference temperature (°C)	1550
Minimum viscosity (Poise)	1.00×10^{19}

2.3. Numerical Approach

The program Picses2D was used for all numerical modeling, and results from Picses2D are published for the first time here. Picses2D operates similar to the geodynamic code FANTOM [*Thieulot*, 2011], and was written nearly simultaneously but independently from FANTOM, with no collaboration between their creators. Interested readers are referred to *Thieulot* [2011] for a full explanation of numerical methods. What follows includes a review of fundamental concepts including all significant differences between Picses2D and FANTOM, primary among those are that Picses2D has a mechanism which simulates phase changes.

Picses2D is an arbitrary Lagrangian-Eulerian (ALE) finite element program that solves the Stokes flow problem (7) in 2D for linear viscous, power-law viscous, and plastic rheologies, with heat conduction within a quasi-rectangular model region. Materials and the evolution of state variables are tracked using the particle-in-cell technique, where Lagrangian material particles (sometimes called “markers” or “tracers”), are advected amidst an Eulerian grid. Particles carry 15 properties with them; some are for calculations and others are assigned from integration points to the particles for visualization purposes. A free upper surface allows for formation of topography. The

vertical column of nodes may deform to account for surface topography, while the horizontal location stays static to avoid overly deforming the mesh. Non-linear materials require iterative solving of the system.

Picses2D operates by first reading user input files, which include a binary file with initial placement of all particles and associated material with the initial geotherm, and another file containing material properties and constants. After reading files, memory is allocated and the stiffness grid is initialized. The code iterates until convergence is reached or an user-spcified number of iterations have occurred before advecting particles and updating the free surface for topography. A time step flows in the following order:

1) New source particles are introduced into the user defined quadrilateral at random x and y locations,
2) Velocity calculation is performed and iterated for convergence,
3) Heat is generated and conducted,
4) Particles are advected with nodal velocities,
5) Mesh and topography are updated, with new Y locations based on advected particle locations,
6) Particles are sorted into finite element cells,
7) Particle stress, strain, pressure, and temperature state is updated,
8) Phase and melt of particles are computed and applied,
9) Transfer of material properties information from atoms back to nodes is made.

Phase changes are accounted for by checking each particle's temperature, pressure, and material type, and computing the current phase from published phase diagrams for a given material type. If the phase is pure melt, it is assigned the melt

density for that material and becomes linear viscous, with the minimum allowed viscosity set by the user, which is 1 x 10^{17} Poise for my models. If the particle is partially melted, density and viscosity are interpolated between values that correspond to complete melt and complete solid. Actual basalt melt viscosity is about 10 orders of magnitude smaller than modeled here [*Wada*, 1994] but, due to numerical range limitations in numerical modeling, the minimum viscosity is limited to ~1 x 10^{17} Poise. This approximation is adequate because the modeled melt viscosity is much lower (> 2 orders of magnitude) than other materials, and still behaves like basaltic melt, flowing much more readily than other materials in the model. This means that actual melt would create longer intrusive features than modeled here. Picses2D does not allow for mode I fractures (an open fracture), the primary means whereby basaltic magma intrudes continental crust, and therefore cannot model melt-filled dikes. Instead of attempting to model dikes with their complexities, the current style of intrusion possible in Picses2D provides a lower limit on intrusion, where actual basaltic melt would create a more extensive and longer dike network. Similar methods for approximating dikes have been used in the past [*Wallner and Schmeling*, 2010].

2.4. Initial Model setup

A 1000-km-wide by 400-km-deep model of a generalized volcanic rifted margin is used (Figure 2). Finite element mesh spacing is 2 x 2 km throughout. Lagrangian particles are placed uniformly every 0.4 km throughout the entire model, initially comprising a total of 2.5 x 10^6 particles. The model initiates with a mass of basaltic, include a free surface on top of the model that allows for topography and free slip on the bottom, left, and right model edges. The base of the model is held at 1,700°C; the top is

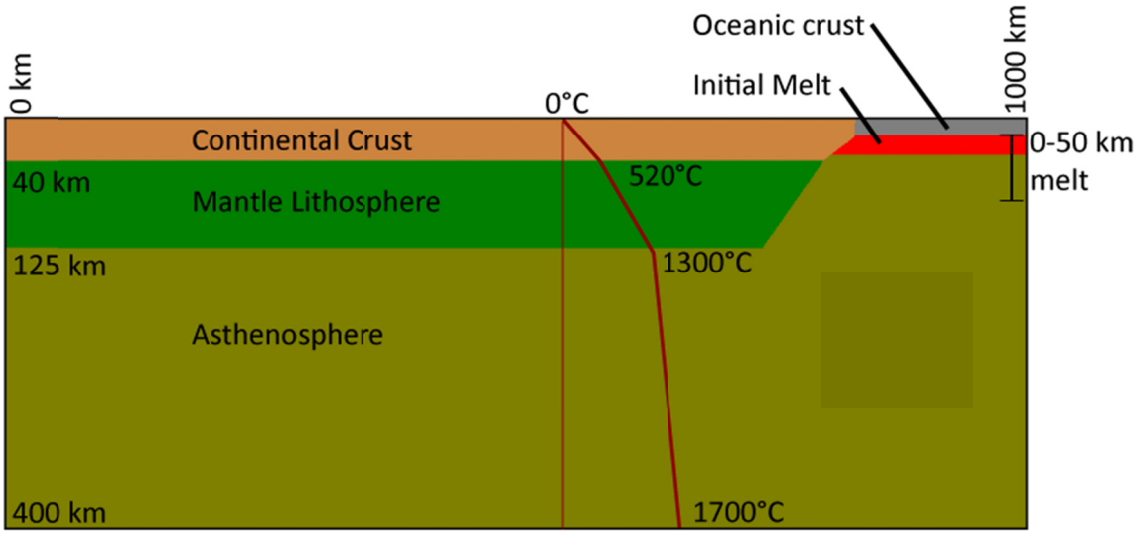

Figure 2. Initial model geometry and geotherm. "Melt" refers to basalt melt from decompressional melting of the asthenosphere, the bulk of which starts off as partial or complete melt. Melt initial thickness is varied from 0-50 km and raised 300°C above the geotherm. Material properties are described in Tables 2-4.

held at 0°C; right and left sides allow no flow of heat outside of the model. The initial geotherm is of young rifted oceanic crust on the right and 40 km thick Phanerozoic continental crust on the left (Figure 2). Most of the extension in continental crust at volcanic passive margins is accomplished by dike intrusion [*Franke*, 2013], and the ocean-continent boundary tends to be sharp, resulting in continental crust a short distance away from the rift that is not especially thin, unlike magma-starved margins [*Franke*, 2013].

The model contains two zones, continental lithosphere (left) and young oceanic lithosphere formed from rifting (right). The continental lithosphere is composed of continental crust, modeled with visco-plastic rheology which includes a ductile lower crust, and sub-crustal lithosphere, modeled with a similar visco-plastic rheology at shallow depths but which changes to simple diffusion creep at depths greater than 130

km. Oceanic crust is modeled with a simple power-law rheology. Asthenosphere is linear viscous (Table 2; Table 4). Pure melt is modeled as linear viscous, and may change phases to solid power-law basalt or eclogite based on phase change rules.

The lithosphere stays cohesive at depth, and is modeled with diffusion creep under asthenospheric pressures and temperatures, because dislocation creep (power-law) becomes too weak (Table 3). The asthenosphere is modeled as linear viscous; attempts at modeling it with diffusion creep gives poor results near the surface (unrealistically strong), particularly in the area of study, where delamination is occurring. The asthenosphere and its convection is not the primary focus of this study, and the linear viscous approximation provided reasonably similar results in comparison testing. An alternative method is to use dislocation creep, but with an upper limit on the asthenosphere viscosity in shallow regions [*Valera et al.*, 2011].

Several crustal power-law rheologies were used: diorite, quartz, wet quartzite, dry granite, wet granite, wet diorite, and a two layer crust of wet quartzite upper crust and plagioclase An_{75} lower crust. All rheologies besides wet granite result in a lower crust that is too strong for intrusion of melt and delamination. The crustal geotherm cools over time, which tends to over-estimate the strength of the crust after the first 0.5 million years (m.y.). Instead of compensating by over-estimating heat production in the crust or starting with a hot crustal geotherm, wet granite rheology is used, which approximates the strength of a hot crustal geotherm. Delamination is known to require high Moho temperatures (~800°C) to create sufficient weakness in the lower crust [*Morency and Doin*, 2004].

Table 4. Flow parameters for power-law creep materials.

Material	A (Pa^{-n} s^{-1})	n	Ea (kJ Mol^{-1})
Dry Olivine [*Ranalli*, 1995]	2.50×10^{17}	3.5	532
Plagioclase An75 [*Ueda et al.*, 2012]	4.80×10^{22}	3.2	238
Wet Granite [*Ranalli*, 1995]	7.76×10^{16}	1.9	137
Wet Quartzite [*Ueda et al.*, 2012]	1.97×10^{17}	2.3	154

Models with wet granite crustal rheology were then created with varying thicknesses of initial melt, from 0-50 km, to represent the variety of margin types, from magma-starved to magma-rich. The rate of additional mafic material supplied beyond the initial thickness was also varied between model runs, from 0-40 material particles per time step, with new particles added every 8000 years (one time step), starting at 0.16 m.y. stopping at ~8 million years. This equates to an increase of .064% of mafic material in the region per time step, or 6.4% over 800,000 years for the typical case of 10 particles added per time step, and 0.256% increase of particles in the region per time step for the case of 40 particles added per step. New cell particles were inserted at random locations near the area of initial melt supply, 5-30 km below the oceanic crust. The material added initiates as melt, basalt, or eclogite, depending on the initial PT conditions of the particle. This addition of material is inferred to be a result of continued decompressional melting of hot asthenosphere rising from depth to replace the asthenosphere flowing into the delamination wedge. As a portion of the hot asthenosphere decompressionally melts near the surface (below the oceanic crust) it creates a positive feedback loop: as melt migrates toward the wedge, more melt is generated below the oceanic crust, thus creating a constant supply of melt. The duration of this feedback mechanism in nature is uncertain, but in the model it continues for ~8 million years.

3. Results

Model results can be grouped into three categories, complete sub-crustal lithosphere removed by delamination, partial removal of the sub-crustal lithosphere by delamination, and no delamination. Models with initial melt thickness of 50 km result in complete removal of the sub-crustal lithosphere by delamination. Models with initial melt thickness of 20-40 km, regardless of rate of mafic material added, show partial removal of the sub-crustal lithosphere. Models with 10 km of initial melt or no melt result in no delamination. Delamination in all models occurs by retreating delamination, where sub-crustal lithosphere detaches from the crust at a migrating delamination hinge, terms defined by *Krystopowicz and Currie* [2013].

In all models that show any type of delamination, the initial melt flattens and begins to intrude the weak lower crust (Figure 3). Intrusion proceeds, but is slowed by a phase change from melt to basalt at the fault tip, where hot melt contacts cool continental lithosphere. Eventually the melt supply runs out, and asthenosphere follows the melt into the decoupled zone. A wedge of mafic material intrudes and decouples the lower crust from the sub-crustal lithosphere. The wedge tip proceeds as long as sufficient melt is available behind it, but progress slows as more melt cools and solidifies to basalt, and then eclogite in the tip. The tip remains as eclogite, with a layer of basalt behind it, followed by partial melt (Figure 4). Once the mafic material runs out, the wedge progress is slowed, but may continue to propagate as the sub-crustal lithosphere is dragged downwards by the already-delaminated portion. By the time this happens, the propagating mafic wedge has been replaced with asthenosphere, and the mafic material is distributed across the base of the crust in a thin layer. The decoupled sub-crustal

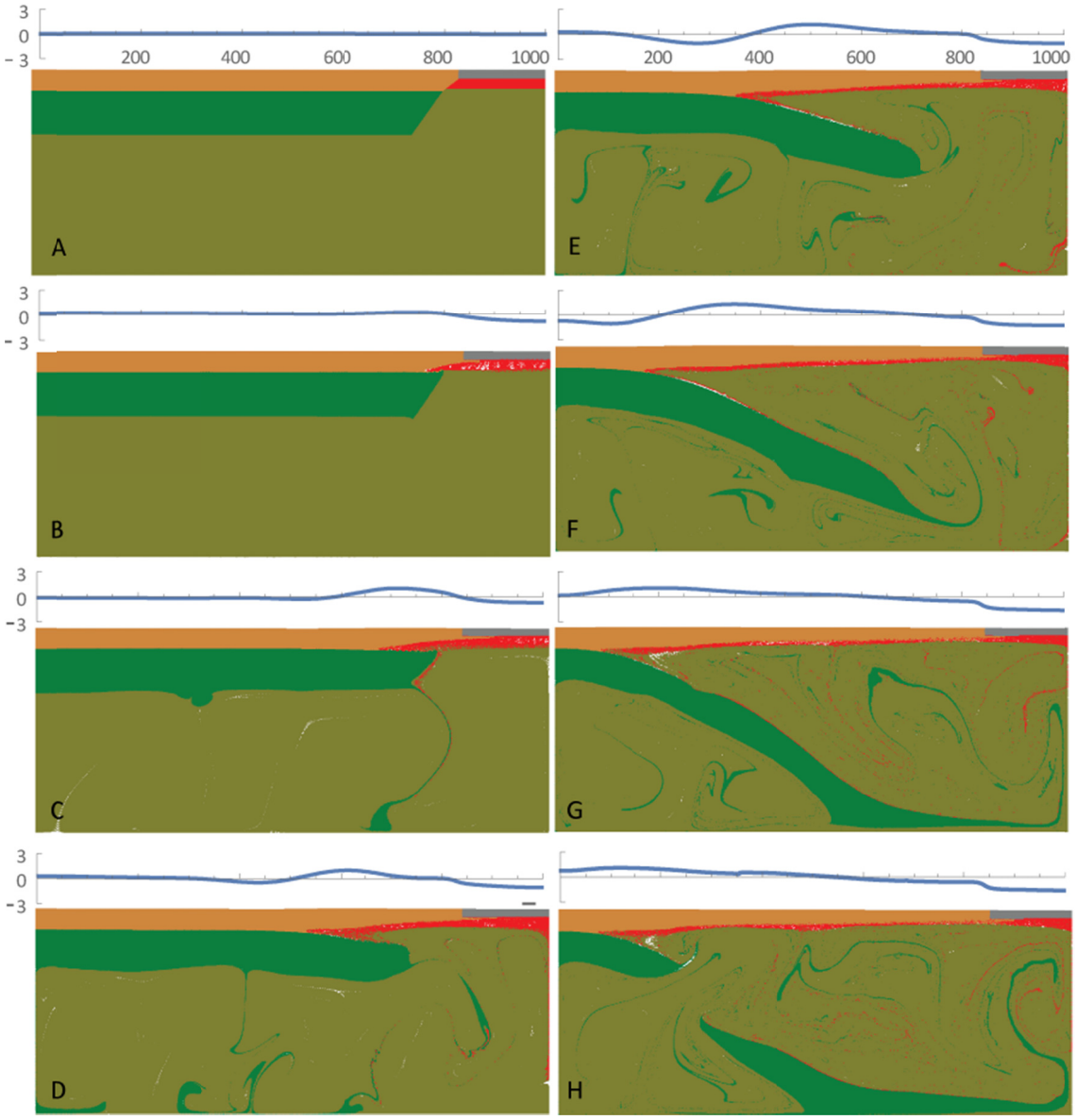

Figure 3. Delamination progression through time of model G2.4 (20 km initial melt, 40 particles per step added). Topographic profiles (km) are shown with the graph above each lithology cross section panel. Mafic material is shown in red, but phase is not shown (any given particle might be melt, basalt, or eclogite depending on PT conditions at location). Green is sub-crustal lithosphere, orange is continental crust, gray is basalt, olive is asthenosphere. Time at each figure is as follow: A – 0 m.y.; B – 0.3 m.y.; C – 1.7 m.y.; D – 7.7 m.y.; E – 12.5 m.y.; F – 16.0 m.y.; G – 21.3 m.y.; H – 23.7 million years.

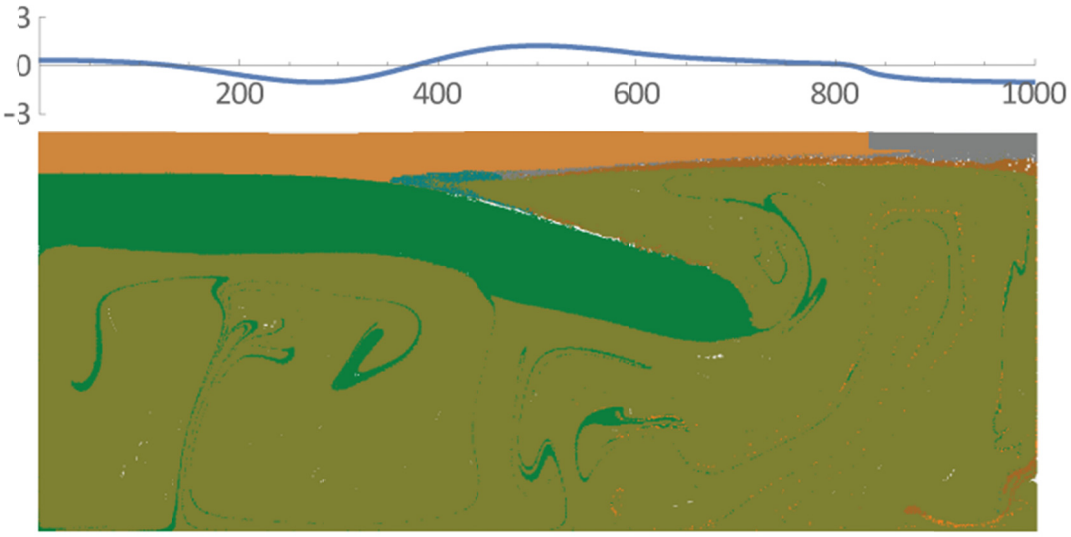

Figure 4. Same as figure 3E, but includes phase of mafic material. Gray is basalt, turquoise is eclogite, brown is partial basalt melt, and orange is pure basalt melt. Eclogite (turquoise) is in the tip of the wedge, followed by basalt (gray) and partial melt (brown).

lithosphere carries small portions of mafic material on its upper surface, typically eclogite, as it sink into the asthenosphere, slowly reaching a state of thermo-equilibrium. As asthenosphere is pulled into the delaminating wedge behind the melt, it pulls hot asthenosphere from depth to replace it. In the case of no melt, a small portion of the lower crust is intruded by asthenospheric material, but no significant change occurs otherwise. When 10 km of initial melt is included, with a rate of additional melt at 10 particles per time step, melt intrudes into the lower crust, and the edge of the sub-crustal lithosphere is decoupled from the crust in a small area, but the lithosphere strength is not overcome and no delamination occurs. The melt becomes an underplate of basalt and eclogite (Figure 5).

Throughout all models, small convection cells develop in the asthenosphere, which heat the base of the ocean crust and continental lithosphere. In between these convection cells Rayleigh Taylor instabilities occur and small portions of the lithosphere

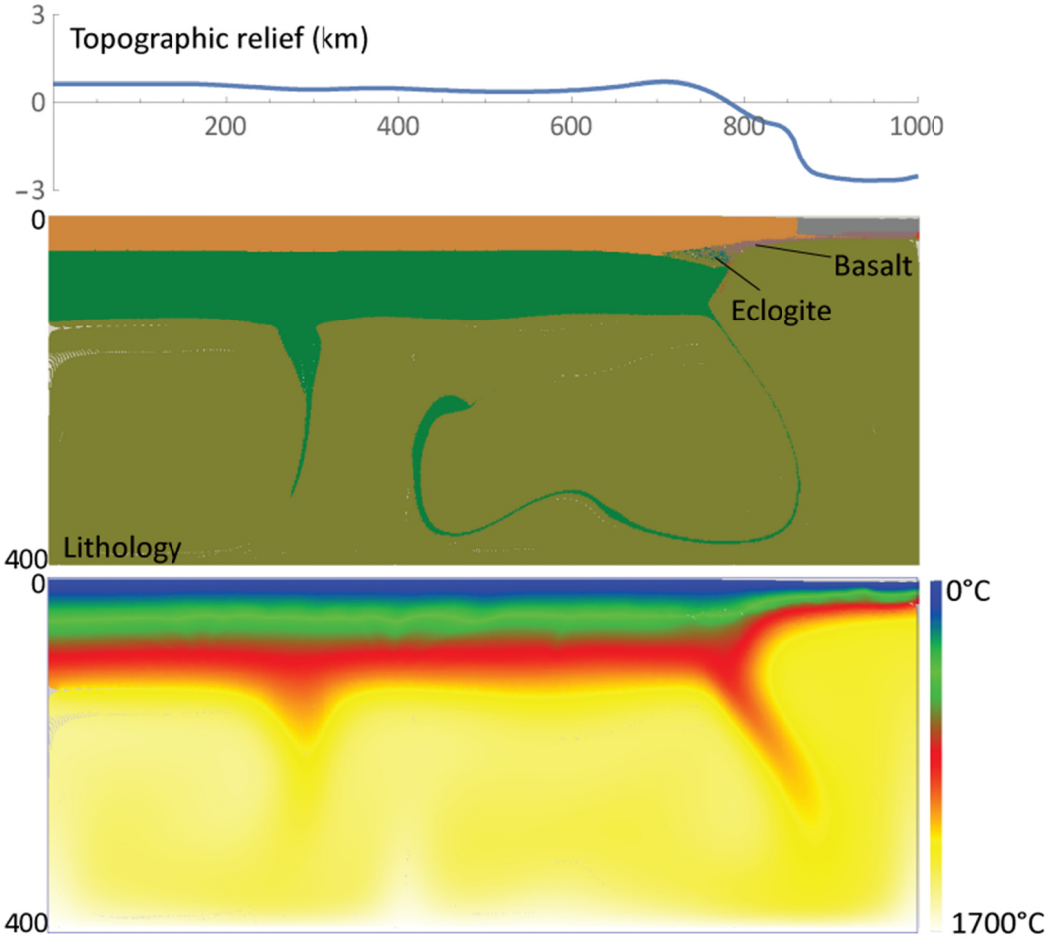

Figure 5. Model G1.1 (10 km of initial melt, 10 particles added per time step) at 20.4 m.y., melt has accumulated along the base of the oceanic and continental crust, changed to basalt and eclogite. Some drips off the lower lithosphere have advected temperature anomalies with them. No delamination has occurred, but a mafic underplate has been emplaced. Topographic relief (10x vertical exaggeration) shows slight uplift associated with ocean-continent transition zone.

are eroded, forming drips into the asthenosphere, where they are heated and become incorporated into the convecting asthenosphere.

Model topography shows the oceanic crust starts out initially at low elevation, with the continental crust having very little relief. Once delamination begins, uplift occurs directly below the delaminated sub-crustal lithosphere. As the delamination hinge

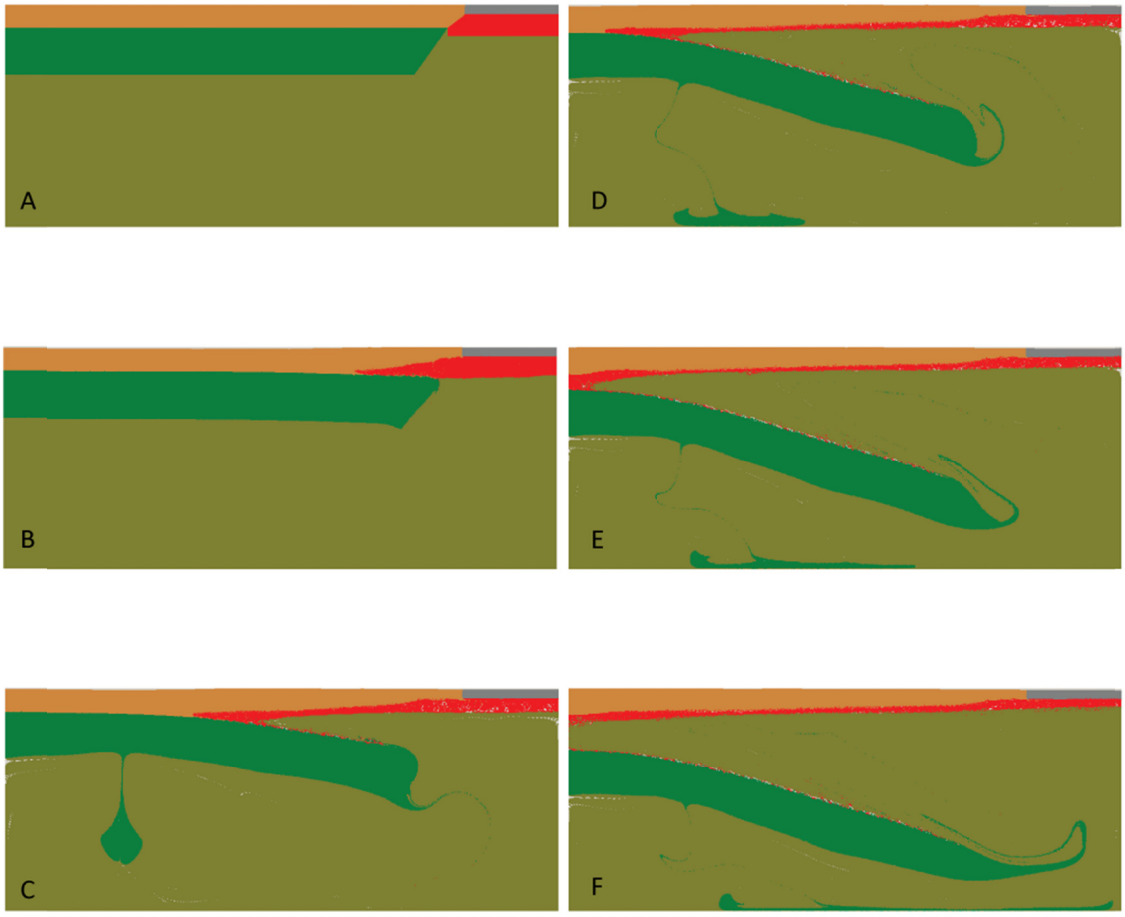

Figure 6. Model G5.1 (50 km initial melt, 10 particles per time step) time series. Colors are the same as figures 1 and 3. Once sub-crustal lithosphere is completely detached, the model becomes unrealistic, but the sub-crustal lithosphere would instead be attached to more landward sub-crustal lithosphere. Time at each figure is as follow: A – 0 m.y.; B – 0.5 m.y.; C – 3.4 m.y.; D – 5.8 m.y.; E – 6.6 m.y.; F – 7.3 million years

propagates into the continent, the peak uplift propagates into the continent along with it. Once an area is uplifted, and the hinge and melt is past, it subsides, but not back to the original elevation (Figure 3).

The model with the maximum amount of initial melt, 50 km, ended in complete delamination of the sub-crustal lithosphere to the left boundary of the model space (Figure 6). It showed the same evolution as models with less initial melt, only preceded faster. This demonstrates the strong control of initial melt on delamination speed. Once

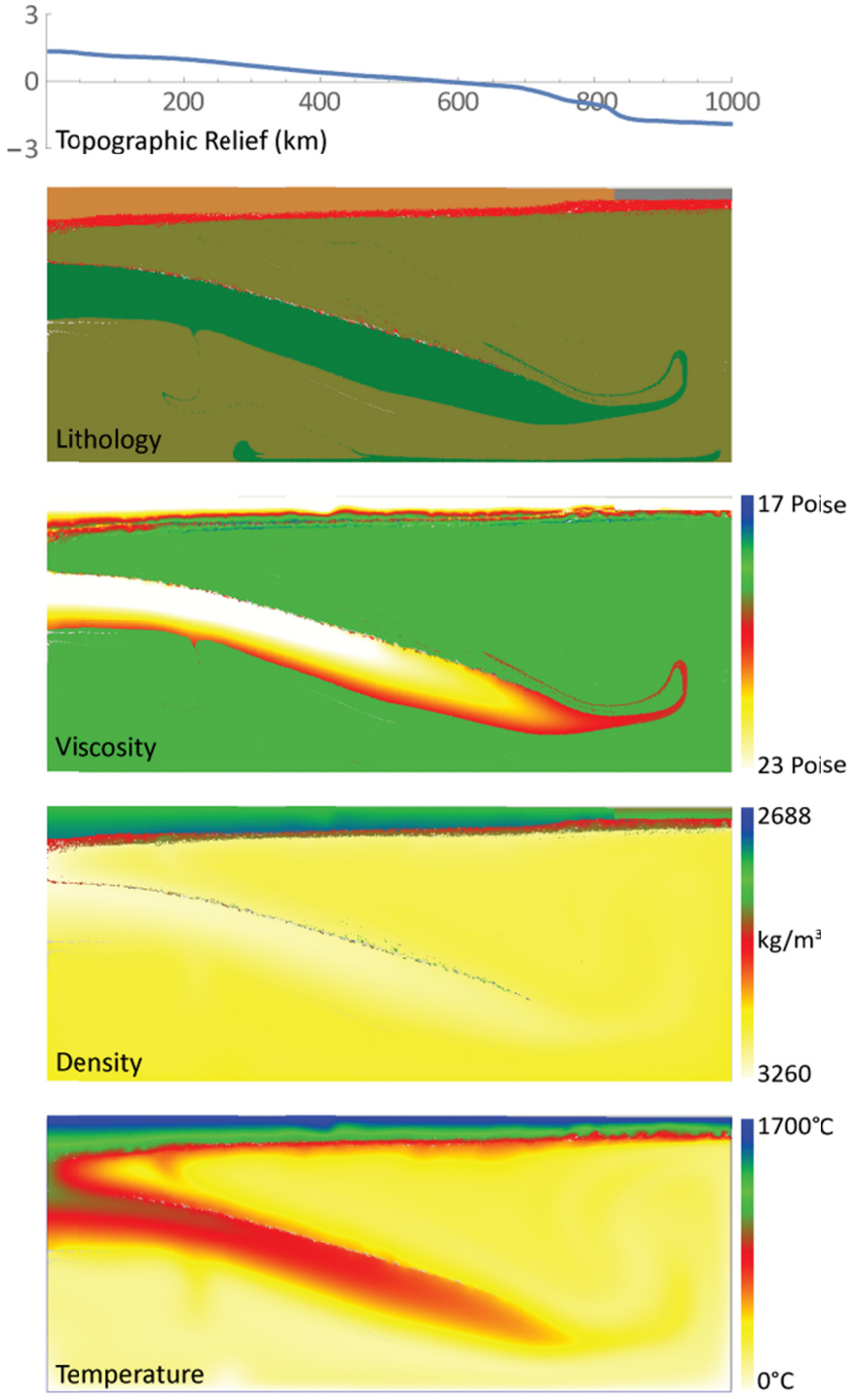

Figure 7. Model G5.1 (50 km initial melt, 10 particles per time step) at 7.3 million years (same as figure 6F). The sub-crustal lithosphere is completely detached from the continental crust, with some mafic material being pulled down on the base of the sub-crustal lithosphere, and the remainder forming a mafic underplate.

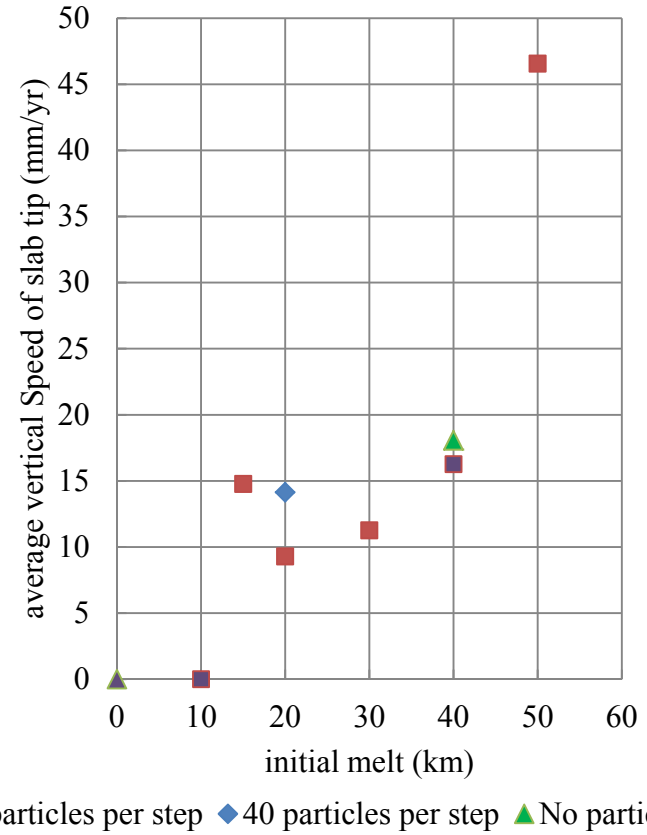

Figure 8. Sensitivity test, points represent different model runs. The average vertical speed of slab tip was used as a proxy for delamination rate. Models with an average vertical speed of 0 indicate no delamination occurred. Average vertical speeds are strongly affected by the initial melt present, and to a lesser degree, by the rate of material particles added per time step. Points in purple have the same number of particles per step as shapes in legend, but asthenosphere viscosity is at 1 x 10^{20} instead of 1 x 10^{19} like all other models.

delamination reaches the model edge, the sub-crustal lithosphere is no longer supported, and the model becomes unrealistic (Figure 7). In reality, the detached lithosphere is always supported by a continuous slab of attached lithosphere more landward of the model until it breaks off. Parameter sensitivity analysis reveals that the most important controlling factor is the strength of lower crust, which must be weak enough that melt can intrude, or instead of decoupling crust from sub-crustal lithosphere, the melt forms an underplate at the continent ocean transition zone with a small amount of intrusion into the

continental crust. The amount of initial melt present has a strong effect on the delamination rate and amount of total delamination that occurs, whereas the rate at which mafic material particles are added has a lesser effect (Figure 8). To ensure all models had a weak lower crust (determining crustal weakness needed for delamination is not the intent of the study), a wet granite rheology was used for all models in the sensitivity study, as mentioned previously. A relatively large amount of mafic material added to the model allows delamination to move further landward than models with no mafic material added. Further weakening the lower crust (either by different crustal rheology or increased temperature) might allow delamination to occur without intrusion of melt, but is beyond the scope of this study.

4. Discussion

Delamination modeled in this study is similar in timing and end result to delamination modeled by others, but the mechanism (emplacement of a mafic underplate in the lower crust) and setting (passive margin) are different [*Morency and Doin*, 2004; *Göğüş and Pysklywec*, 2008a; *Pysklywec et al.*, 2010; *Ueda et al.*, 2012; *Krystopowicz and Currie*, 2013]. Estimates of the rate of delamination and the time from initiation to complete detachment of the sub-crustal lithosphere also vary, but both rate and times of the modeling results of others appear to be similar to results of this study [*Morency and Doin*, 2004; *Krystopowicz and Currie*, 2013].

With poorly constrained input parameters- and the right starting model, geodynamic models can simulate nearly any described, real or imagined, geologic phenomena. To limit modeling closer to reality, unnatural boundary conditions (not found in nature), and initial starting models can be separated as far as possible from the

model area of interest. In the case of necessary boundary conditions, the separation is spatial. The model space may be expanded so the model borders are far from the study area of interest. The initial model can be "pushed back" in time, meaning the initial model may be very unlike the final result, showing the result is robust and can occur on its own, without starting with an unlikely set of initial conditions. In the case of geodynamic modeling of delamination, this has been achieved by allowing the delamination to self-propagate, with no initial weakness in the lithosphere [*Morency and Doin*, 2004], or in the case of delamination of a orogenic root, models begin with no relief or orogenic root and the formation of an orogeny is modeled, as opposed to starting with a thick and dense orogenic root [*Ueda et al.*, 2012; *Krystopowicz and Currie*, 2013]. The initial models considered in the current study begin with melt leftover from passive rifting, before formation of an underplate in an otherwise stable rift zone. "Push back" the initial model in time, future models could began with a pre-rift formation.

My models show intrusion of mafic melt as an underplate at the Moho, between the lower crust and sub-crustal lithosphere. Underplated regions with similar geometries have been observed both at volcanic margins, such as Vøring and North Atlantic margins, and also magma-poor margins, such as West Antarctica. *Wobbe et al.* [2012] interpret that the rifted margin of West Antarctica shows evidence of a dense (3000 g km^{-3}) wedge shaped mafic underplate between the lower crust and lithosphere, the tip extending to the edge of the continent-ocean transition zone, about 620 km from the oceanic crust. Being a typical magma-poor margin, the melt below most of the continent ocean transition zone is ~5 km thick, and thins to a tip. The remaining melt below the oceanic crust is about 8-10

km thick. The Vøring margin has an underplate >10 km thick in places, which likely contains partially eclogitized mafic material [*Mjelde et al.*, 2009].

Successful models of delamination contain a broad region of uplift above the zone of missing sub-crustal lithosphere, as expected from delamination [*Schott and Schmeling*, 1998; *Göğüş and Pysklywec*, 2008b]. Many passive margins around the world are elevated 1-2 km above sea level [*Weissel and Karner*, 1989]. Some suppose this uplift occurred in relation to rifting [*Weissel and Karner*, 1989], and that little erosion has taken place since, while others infer the margins have been uplifted long after rifting has finished [*Japsen et al.*, 2012]. Models with delamination show uplift occurring concurrently with removal of the sub-crustal lithosphere by delamination, which begins after, or at the end of, the rifting process. The results of the current study show that post-rift uplift of passive margins could have been caused by delamination of the sub-crustal lithosphere.

The idea of rift-induced delamination has previously been modeled in an area of continental rifting [*Wallner and Schmeling*, 2010] by a mechanism of parallel intrusion of asthenospheric material into the lower crust at offset rift segments followed by intrusion and heating of the lower crust, which decouples the crust from the sub-crustal lithosphere and allows for vertical sinking of a block of sub-crustal lithosphere (Figure 9). This pincer-like mechanism for vertical delamination is reminiscent of the vertical delamination in zones of extension hypothesized by Meissner and Mooney [1998]. However, such a mechanism is unlikely to cause large-scale delamination, as appears to have happened in the Basin and Range. Aside from taking advantage of the thinned sub-crustal lithosphere in rift zones for initiation of delamination, the overall mechanisms of

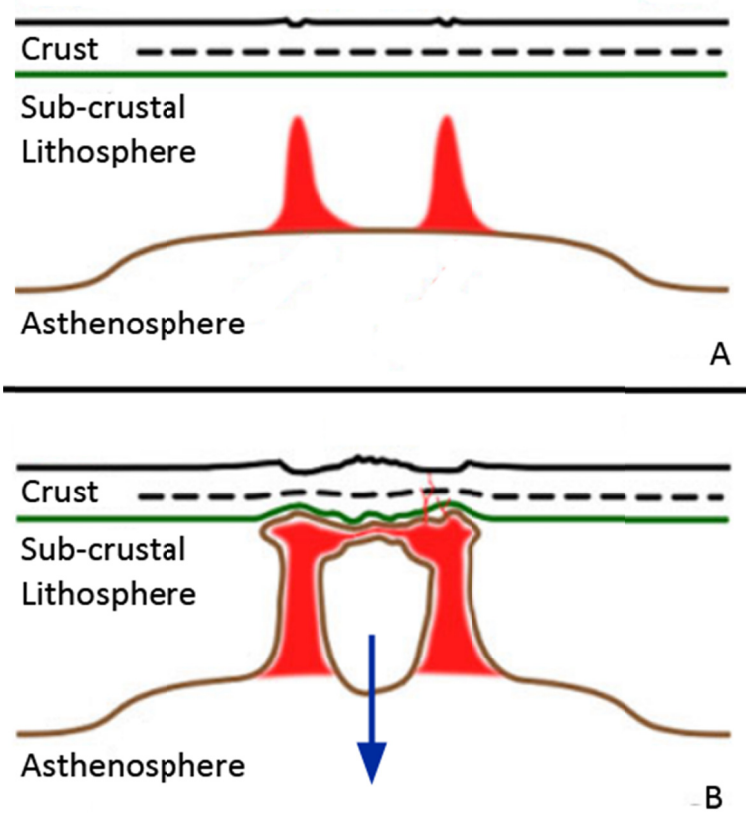

Figure 9. Rift induced delamination below the Rwenzori Mountains, another style of delamination in a region of extension. Asthenosphere heats up and intrudes the sub-crustal lithosphere, and dikes form in the lower crust, decoupling a block of sub-crustal lithosphere. The resulting isostatic pop-up may have created the high topography of the Rwenzori Mountains. After Wallner and Schmeling [2010].

delamination are otherwise different from the current study, although both show delamination is plausible in a regime of extension.

As noted by *Mickus et al.* [2009] the Texas portion of the Gulf of Mexico margin appears to contain a deeply buried volcanic rifted margin. The magnetic and gravity anomalies associated with this volcanic rift are comparable to those of other volcanic rifted margins (Namibia). The thickness of the volcanic rifted margins varies from ~25-15 km thick below Jurassic and younger sediments. This opens the possibility that volcanism form this volcanic rifted margin may have led to delamination of sub-crustal

lithosphere as modeled in the current study. If delamination occurred, it would have caused increased heat flow in the crust than other wise expected.

5. Concluding Remarks

This is the first study to model delamination at a passive margin. Using a finite element code, Picses2D, I have found that when the lower crust is weak, mafic material can intrude into and decouple the sub-crustal lithosphere from the crust, causing the initiation of delamination. Once initiated, the underplate material continues to decouple the crust, while the sub-crustal lithosphere delaminates under its own negative buoyancy. The presence of greater volume of melt causes the delamination to propagate farther landward. Once melt is no longer supplied, the delaminated slab eventually breaks off and sinks into the asthenosphere. In our modeling, initial melt thickness less than 10 km did not initiate delamination, while initial melt thicknesses of at least 20 km created large (> 200 km long) delamination events.

References

Anderson, D. L. (2007), *New theory of the Earth*, Cambridge University Press, Cambridge, UK ; New York.

Arnold, J., W. R. Jacoby, H. Schmeling, and B. Schott (2001), Continental collision and the dynamic and thermal evolution of the Variscan orogenic crustal root — numerical models, *J. Geodyn.*, *31*(3), 273–291.

Bajolet, F., J. Galeano, F. Funiciello, M. Moroni, A.-M. Negredo, and C. Faccenna (2012), Continental delamination: Insights from laboratory models, *Geochem. Geophys. Geosystems*, *13*(2), n/a–n/a, doi:10.1029/2011GC003896.

Bezada, M. J., E. D. Humphreys, J. m. Davila, R. Carbonell, M. Harnafi, I. Palomeras, and A. Levander (2014), Piecewise delamination of Moroccan lithosphere from beneath the Atlas Mountains, *Geochem. Geophys. Geosystems*, *15*(4), 975–985, doi:10.1002/2013GC005059.

Bird, P. (1978), Initiation of intracontinental subduction in the Himalaya, *J. Geophys. Res.*, *83*(B10), 4975–4987, doi:10.1029/JB083iB10p04975.

Bird, P. (1979), Continental delamination and the Colorado Plateau, *J. Geophys. Res. Solid Earth*, *84*(B13), 7561–7571, doi:10.1029/JB084iB13p07561.

Brace, W. F., and D. L. Kohlstedt (1980), Limits on lithospheric stress imposed by laboratory experiments, *J. Geophys. Res. Solid Earth*, *85*(B11), 6248–6252, doi:10.1029/JB085iB11p06248.

Buffett, B. A., and T. W. Becker (2012), Bending stress and dissipation in subducted lithosphere, *J. Geophys. Res.*, *117*(B5), doi:10.1029/2012JB009205.

Burov, E. B. (2011), Rheology and strength of the lithosphere, *Mar. Pet. Geol.*, *28*(8), 1402–1443, doi:10.1016/j.marpetgeo.2011.05.008.

Byerlee, J. (1978), Friction of rocks, *Pure Appl. Geophys.*, *116*(4-5), 615–626.

Calvert, A., E. Sandvol, D. Seber, M. Barazangi, S. Roecker, T. Mourabit, F. Vidal, G. Alguacil, and N. Jabour (2000), Geodynamic evolution of the lithosphere and upper mantle beneath the Alboran region of the western Mediterranean; constraints from travel time tomography, *J. Geophys. Res.*, *105*(B5), 10871–10898, doi:10.1029/2000JB900024.

Channell, J. E. T., and J. C. Mareschal (1989), Delamination and asymmetric lithospheric thickening in the development of the Tyrrhenian Rift, *Geol. Soc. Spec. Publ.*, *45*, 285–302.

Chiarabba, C., and G. Chiodini (2013), Continental delamination and mantle dynamics drive topography, extension and fluid discharge in the Apennines, *Geology*, *41*(6), 715–718, doi:10.1130/G33992.1.

Ducea, M., and J. B. Saleeby (1998), A case for delamination of the deep batholithic crust beneath the Sierra Nevada, California, *Int. Geol. Rev.*, *40*(1), 78–93.

Ducea, M. N. (2011), Fingerprinting orogenic delamination, *Geology*, *39*(2), 191–192, doi:10.1130/focus022011.1.

Fillerup, M. A., J. H. Knapp, C. C. Knapp, and V. Raileanu (2010), Mantle earthquakes in the absence of subduction? Continental delamination in the Romanian Carpathians, *Lithosphere*, *2*(5), 333–340, doi:10.1130/L102.1.

Forsyth, D., and S. Uyedaf (1975), On the Relative Importance of the Driving Forces of Plate Motion, *Geophys. J. R. Astron. Soc.*, *43*(1), 163–200, doi:10.1111/j.1365-246X.1975.tb00631.x.

Franke, D. (2013), Rifting, lithosphere breakup and volcanism: Comparison of magma-poor and volcanic rifted margins, *Mar. Pet. Geol.*, *43*, 63–87, doi:10.1016/j.marpetgeo.2012.11.003.

Funck, T., H. R. Jackson, and J. Shimeld (2011), The crustal structure of the Alpha Ridge at the transition to the Canadian Polar Margin: Results from a seismic refraction experiment, *J. Geophys. Res. Solid Earth*, *116*(B12), B12101, doi:10.1029/2011JB008411.

Fyfe, W. S. (1992), Magma underplating of continental crust, *J. Volcanol. Geotherm. Res.*, *50*(1–2), 33–40, doi:10.1016/0377-0273(92)90035-C.

Geoffroy, L. (2005), Volcanic passive margins, *Comptes Rendus Geosci.*, *337*(16), 1395–1408, doi:10.1016/j.crte.2005.10.006.

Gerya, T. V. (2010), *Introduction to Numerical Geodynamic Modelling*, Cambridge University Press.

Giacomuzzi, G., C. Chiarabba, and P. De Gori (2011), Linking the Alps and Apennines subduction systems: New constraints revealed by high-resolution teleseismic tomography, *Earth Planet. Sci. Lett.*, *301*(3–4), 531–543, doi:10.1016/j.epsl.2010.11.033.

Göğüş, O. H., and R. N. Pysklywec (2008a), Mantle lithosphere delamination driving plateau uplift and synconvergent extension in eastern Anatolia, *Geology*, *36*(9), 723–726, doi:10.1130/G24982A.1.

Göğüş, O. H., and R. N. Pysklywec (2008b), Near-surface diagnostics of dripping or delaminating lithosphere, *J. Geophys. Res. Solid Earth*, *113*(B11), n/a–n/a, doi:10.1029/2007JB005123.

Houseman, G. A., D. P. McKenzie, and P. Molnar (1981), Convective instability of a thickened boundary layer and its relevance for the thermal evolution of continental convergent belts, *J. Geophys. Res. Solid Earth*, *86*(B7), 6115–6132, doi:10.1029/JB086iB07p06115.

Japsen, P., J. A. Chalmers, P. F. Green, and J. M. Bonow (2012), Elevated, passive continental margins: Not rift shoulders, but expressions of episodic, post-rift burial and exhumation, *Glob. Planet. Change*, *90–91*, 73–86, doi:10.1016/j.gloplacha.2011.05.004.

Jull, M., and P. B. Kelemen (2001), On the conditions for lower crustal convective instability, *J. Geophys. Res. Solid Earth*, *106*(B4), 6423–6446, doi:10.1029/2000JB900357.

Kameyama, M., D. A. Yuen, and S.-I. Karato (1999), Thermal-mechanical effects of low-temperature plasticity (the Peierls mechanism) on the deformation of a viscoelastic shear zone, *Earth Planet. Sci. Lett.*, *168*(1–2), 159–172, doi:10.1016/S0012-821X(99)00040-0.

Kay, R. W., and S. Mahlburg-Kay (1991), Creation and destruction of lower continental crust, *Geol. Rundsch.*, *80*(2), 259–278, doi:10.1007/BF01829365.

Knapp, J. H., C. C. Knapp, V. Raileanu, L. Matenco, V. Mocanu, and C. Dinu (2005), Crustal constraints on the origin of mantle seismicity in the Vrancea Zone, Romania; the case for active continental lithospheric delamination, *Tectonophysics*, *410*(1-4), 311–323, doi:10.1016/j.tecto.2005.02.020.

Krystopowicz, N. J., and C. A. Currie (2013), Crustal eclogitization and lithosphere delamination in orogens, *Earth Planet. Sci. Lett.*, *361*, 195–207, doi:10.1016/j.epsl.2012.09.056.

Lavier, L. L., and G. Manatschal (2006), A mechanism to thin the continental lithosphere at magma-poor margins, *Nature*, *440*(7082), 324–328, doi:10.1038/nature04608.

Leech, M. L. (2001), Arrested orogenic development: eclogitization, delamination, and tectonic collapse, *Earth Planet. Sci. Lett.*, *185*(1–2), 149–159, doi:10.1016/S0012-821X(00)00374-5.

Meissner, R., and W. Mooney (1998), Weakness of the lower continental crust: a condition for delamination, uplift, and escape, *Tectonophysics*, *296*(1), 47–60.

Mickus, K., R. J. Stern, G. R. Keller, and E. Y. Anthony (2009), Potential field evidence for a volcanic rifted margin along the Texas Gulf Coast, *Geology*, *37*(5), 387–390.

Mjelde, R., J. I. Faleide, A. J. Breivik, and T. Raum (2009), Lower crustal composition and crustal lineaments on the Vøring Margin, NE Atlantic: A review, *Tectonophysics*, *472*(1–4), 183–193, doi:10.1016/j.tecto.2008.04.018.

Morency, C., and M.-P. Doin (2004), Numerical simulations of the mantle lithosphere delamination, *J. Geophys. Res. Solid Earth*, *109*(B3), n/a–n/a, doi:10.1029/2003JB002414.

Poudjom Djomani, Y. H., S. Y. O'Reilly, W. L. Griffin, and P. Morgan (2001), The density structure of subcontinental lithosphere through time, *Earth Planet. Sci. Lett.*, *184*(3–4), 605–621, doi:10.1016/S0012-821X(00)00362-9.

Pysklywec, R. N., O. Gogus, J. Percival, A. R. Cruden, and C. Beaumont (2010), Insights from geodynamical modeling on possible fates of continental mantle lithosphere: collision, removal, and overturn, *Can. J. Earth Sci.*, *47*(4), 541–563, doi:10.1139/E09-043.

Ranalli, G. (1995), *Rheology of the Earth*, Springer Science & Business Media.

Ren, Y., and Y. Shen (2008), Finite frequency tomography in southeastern Tibet: Evidence for the causal relationship between mantle lithosphere delamination and the north–south trending rifts, *J. Geophys. Res. Solid Earth*, *113*(B10), n/a–n/a, doi:10.1029/2008JB005615.

Rudnick, R. L. (1995), Making continental crust, *Nature*, *378*(6557), 571–578, doi:10.1038/378571a0.

Schott, B., and H. Schmeling (1998), Delamination and detachment of a lithospheric root, *Tectonophysics*, *296*(3), 225–247.

Scrutton, R. A. (1982), Passive continental margins: A review of observations and mechanisms, in *Dynamics of Passive Margins*, edited by R. A. Scrutton, pp. 5–11, American Geophysical Union.

Seber, D., M. Barazangi, A. Ibenbrahim, and A. Demnati (1996), Geophysical evidence for lithospheric delamination beneath the Alboran Sea and Rif-Betic mountains, *Nat. Lond.*, *379*(6568), 785–790.

Semprich, J., and N. S. C. Simon (2014), Inhibited eclogitization and consequences for geophysical rock properties and delamination models: Constraints from cratonic lower crustal xenoliths, *Gondwana Res.*, *25*(2), 668–684, doi:10.1016/j.gr.2012.08.018.

Thieulot, C. (2011), FANTOM: Two- and three-dimensional numerical modelling of creeping flows for the solution of geological problems, *Phys. Earth Planet. Inter.*, *188*(1-2), 47–68, doi:10.1016/j.pepi.2011.06.011.

Thybo, H., and I. M. Artemieva (2013), Moho and magmatic underplating in continental lithosphere, *Tectonophysics*, *609*, 605–619, doi:10.1016/j.tecto.2013.05.032.

Tucholke, B. ., D. . Sawyer, and J.-C. Sibuet (2007), Breakup of the Newfoundland-Iberia rift, in *Geological Society Special Publication*, vol. 282, pp. 9 – 46.

Ueda, K., T. V. Gerya, and J.-P. Burg (2012), Delamination in collisional orogens: Thermomechanical modeling, *J. Geophys. Res. Solid Earth*, *117*(B8), n/a–n/a, doi:10.1029/2012JB009144.

Valera, J.-L., A.-M. Negredo, and A. Villaseñor (2008), Asymmetric Delamination and Convective Removal Numerical Modeling: Comparison with Evolutionary Models for the Alboran Sea Region, *Pure Appl. Geophys.*, *165*(8), 1683–1706, doi:10.1007/s00024-008-0395-8.

Valera, J. L., A. M. Negredo, and I. Jiménez-Munt (2011), Deep and near-surface consequences of root removal by asymmetric continental delamination, *Tectonophysics*, *502*(1–2), 257–265, doi:10.1016/j.tecto.2010.04.002.

Wada, Y. (1994), On the relationship between dike width and magma viscosity, *J. Geophys. Res. Solid Earth*, *99*(B9), 17743–17755, doi:10.1029/94JB00929.

Wallner, H., and H. Schmeling (2010), Rift induced delamination of mantle lithosphere and crustal uplift: a new mechanism for explaining Rwenzori Mountains' extreme elevation?, *Int. J. Earth Sci.*, *99*(7), 1511–1524, doi:10.1007/s00531-010-0521-6.

Wallner, H., and H. Schmeling (2011), Sensitivity analysis of rift induced delamination with application to Rwenzori Mountains, *Geophys. J. Int.*, *187*(3), 1135–1145, doi:10.1111/j.1365-246X.2011.05237.x.

Weissel, J. K., and G. D. Karner (1989), Flexural uplift of rift flanks due to mechanical unloading of the lithosphere during extension, *J. Geophys. Res. Solid Earth*, *94*(B10), 13919–13950, doi:10.1029/JB094iB10p13919.

White, R. S., and D. P. McKenzie (1989), Volcanism at Rifts, *Sci. Am.*, *261*(1), 62.

White, R. S. et al. (2008), Lower-crustal intrusion on the North Atlantic continental margin, *Nature*, *452*(7186), 460–464, doi:10.1038/nature06687.

Van Wijk, J., J. Van Hunen, and S. Goes (2008), Small-scale convection during continental rifting: Evidence from the Rio Grande rift, *Geology*, *36*(7), 575–578, doi:10.1130/G24691A.1.

Wobbe, F., K. Gohl, A. Chambord, and R. Sutherland (2012), Structure and breakup history of the rifted margin of West Antarctica in relation to Cretaceous separation from Zealandia and Bellingshausen plate motion, *Geochem. Geophys. Geosystems*, *13*(4), Q04W12, doi:10.1029/2011GC003742.

Zandt, G., H. Gilbert, T. J. Owens, M. Ducea, J. Saleeby, and C. H. Jones (2004), Active foundering of a continental arc root beneath the southern Sierra Nevada in California, *Nature*, *431*(7004), 41–46, doi:10.1038/nature02847.

CHAPTER THREE

Conclusions

This study shows that lithospheric delamination at passive margins is possible under specific conditions. The lower continental crust must be weak, either because of composition or high temperature. Sufficient melt remain after the rifting process to initiate the decoupling of the lower crust from the sub-crustal lithosphere. Additional melt generated by decompressional melting will cause delamination to continue further into the continental lithosphere and delamination to proceed at higher rates. Future work building on this study could include more numerical modeling but could also consist of a search for evidence of delamination under these conditions using geophysical methods, such as seismic and gravity studies.